

Alternative materials to shorten injection mold manufacturing and molding cycles

Adriano Fagali de Souza^{1*} , Janaina Lisi Leite Howarth² , Bruno Edu Arendarchuck¹ ,
Alexandre Mateus Popiolek¹ , Claudio Antonio Treml Junior² and Crislaine Kavilha²

¹*Grupo de Pesquisa em Manufatura Auxiliada por Computador – GPCAM, Laboratório de Mecânica de Precisão – LMP, Departamento de Engenharia Mecânica, Universidade Federal de Santa Catarina – UFSC, Florianópolis, SC, Brasil*

²*Departamento de Engenharia Mecânica, Sociedade Educacional de Santa Catarina – SOCIESC, Joinville, SC, Brasil*

*adriano.fagali@ufsc.br

Abstract

This paper investigates mold materials for polypropylene (PP) injection molding, including CuBe alloy (high thermal conductivity), AISI P20 mold steel (the conventional material for injection molds), and polyurethane resin (rapid tooling). Characterization of molded parts involved microstructural analysis, tensile tests, warping, and degree of crystallinity assessments. The results show that the higher thermal conductivity of the mold's inserts reduced the injection molding cycle time and produced thicker skins, which resulted in smaller spherulite sizes in the core of the samples, reduced the crystallinity degree, and consequently reduced the maximum strain property. The thermal conductivity of the molds' inserts was shown to be more significant than the skin thickness and mold temperature for the size of the spherulites when they are formed. In addition, CuBe alloys showed to be a strong competitor with additive manufacturing-produced molds with conformal cooling channels to reduce injection molding cycle time.

Keywords: *CuBe alloys, injection molding, mold materials, processing cycle time.*

How to cite: Souza, A. F., Howarth, J. L. L., Arendarchuck, B. E., Popiolek, A. M., Treml Junior, C. A., & Kavilha, C. (2024). Alternative materials to shorten injection mold manufacturing and molding cycles. *Polímeros: Ciência e Tecnologia*, 34(2), e20240023. <https://doi.org/10.1590/0104-1428.20230088>

1. Introduction

The injection molding process using polypropylene (PP) material is one of the most popular techniques for fabricating thermoplastic products and components in a vast range of segments such as the medical industry, electronics, goods, automobile, among others^[1]. This process requires a metal mold usually manufactured by machining. AISI P20 steel is mostly used for this application due to its wear resistance, machinability, high polishing capability, and availability on the current market^[2].

The injection molding cycle process includes the following phases: feeding the plastic material, pressurizing and holding, cooling, and ejection of the part from the mold^[3]. Within the process, factors such as injection rate, mold temperature (including cooling phase duration and rate), mold thickness, and the molecular weight of the molding material play crucial roles in determining the morphology and mechanical performance of semicrystalline injection moldings^[4]. It is worth noting that cooling is one of the most important stages of the process because it can deeply affect the production efficiency and the quality of the final parts in terms of mechanical properties and microstructure formation^[5]. A Non-uniform heat transfer during the cooling phase in the molding can also result in warpage and deformations of the

molded parts can also result in warpage and deformations of the molded parts^[6].

During the injection molding process, after the melting phase, the final plastic part is formed by two distinct regions presenting morphological distinctions: an outer region with a highly oriented layer in the border of the material known as *skin*, and a massive region in the central portion known as the *core*. The arrangement of these layers can occur according to the processing parameters, part geometry, mold design, and the molded material's properties^[7]. According to Karger-Kocsis and Bárány^[8], the polypropylene core layer is much thicker than the other layers because the core is cooled down slowly, thus it has more time to crystallize. The thickness of the skins is influenced by the flow rate, the material viscosity, filling time, mold temperature, heat conductivity, melt temperature, cavity thickness, surface roughness, geometry, and mold coating. A thinner skin layer can promote flexibility and resistance to cracking or stress failure^[9]. However, its final size is determined by the degree of relaxation of stress-induced orientation in the material. A shorter cooling time reduces the period for the material to relax its orientation, thereby increasing the 'original' size of the oriented skin^[4].

Processing polymers by injection molding promotes different shear or compressive forces, which can be related to changes in materials features such as degree of crystallinity and crystallization formation^[10,11]. According to Rizvi^[12], higher mold temperature is favorable for yield strength and tensile modulus. Depending on the cooling rate (i.e., mold temperature), the crystallization rate of the polymer is modified as well as its crystalline microstructure and crystallinity percentage^[13]. This mainly occurs during the packing and cooling phase due to its transient nature and the rapid changes in pressure and temperature^[14].

The degree of crystallinity influences the material's longer-range arrangement level. A high degree of crystallinity degree of crystallinity in polymers leads to increased modulus of elasticity and maximum strain^[15]. The high mold temperature prevents the cooling process from rapidly cooling the material, leading it to crystallize fully to its equilibrium state, especially near the sample wall. In experiments with slower flow rates, the flow-induced crystallization (FIC) effect on crystallization kinetics isn't enough to offset the influence of intense cooling. Consequently, the quenching zone thickness increases^[8]. Differential scanning calorimetry (DSC) techniques can be used to evaluate the crystalline degree^[14].

The major effect of crystallites is to act as a cross-linked network. The deformation of polymer – i.e., moving dislocations and the presence of glide planes – are restricted by forming a significant cross-linked network; thus, increasing crystallinity is expected to improve mechanical properties^[16].

Today, one of the efforts expended to develop this manufacturing process concentrates on the reduction of the injection molding cycle time by using materials, instead of AISI P20, with high thermal conductivity to manufacture molds^[17]. Another effort involves focusing on the reduction of the time required to manufacture the injection mold itself by using alternative materials to facilitate the manufacturing of the mold, known as the *rapid tooling approach*^[18]. Taking into account these efforts, the materials used for manufacturing the molds are the issue investigated in the present work.

Some alternative materials with higher thermal conductivity can be used for mold inserts, such as copper-beryllium (CuBe) alloys^[19]. These alloys, with more than 1.7 wt. % of Be, have prevailed in the market because they present adequate mechanical properties, hardening up to 330 to 360 Brinell. In this range, the material is ductile, has no tendency to fragility at the edges, and is readily polishable, which are essential characteristics to produce parts with low degrees of roughness. Machining or casting can be used to produce such molds^[17].

Apacki^[20] and Kelly et al.^[21] evaluated the injection molding cycle time using a mold of CuBe and another fabricated with AISI P20 steel. These results showed a reduction of 17% in the cycle time compared to P20 steel in the first experiment and a reduction of 25% of the cooling time was achieved in the second one. Warpage measurements of the injected parts did not show statistical differences between CuBe and P20 molds. These studies are important contributions to the knowledge of the molding process using CuBe alloy, but it is still missing the analyses of the microstructure skin and the degree of crystallinity degree of crystallinity of

the injected parts in such molds with a higher cooling rate. According to Lee and Cha^[9], there is a lack of knowledge of the factors that influence the formation of the skin layer and its thickness, which can directly impact the properties of the molded parts.

Based on this background, the current work presents an investigation of the microstructure formation and degree of crystallinity degree of crystallinity of polypropylene parts manufactured by injection molding using different materials, with very different thermal conductivity, for the mold's inserts, focusing on: i) rapid tooling approach, and ii) reduction of the injection molding cycle time. To be closer to real application, a free-form workpiece and its molds were designed and manufactured. This workpiece geometry and the mold were originally designed for research purposes and are used in other projects^[22]. Three pairs of mold inserts were manufactured using: i) CuBe alloy (rapid cooling), ii) polyurethane resin (rapid tooling), and iii) AISI P20 steel ordinary material.

Batches of injection molding were conducted altering these three pairs of inserts. The molded workpieces were investigated in terms of microstructure formation, crystallinity degree, warpage, and mechanical properties. CAE simulations were carried out and the real temperature inside the mold was obtained in real-time to contribute to the understanding of the phenomena that occur during these injection molding processes. The experimental procedures are detailed below.

2. Experimental Procedure

A representative workpiece containing free-form geometries was designed and modeled in 3D CAD software. A mold with interchangeable inserts was also designed and manufactured. These inserts were manufactured using the following three different materials: i) ordinary AISI P20 steel, ii) Plasloy 20C a CuBe alloy with Be greater than 1.7% (fast cooling), and iii) Huntsman RenShape®5166 (rapid tooling) – a polyurethane resin matrix reinforced with aluminum trihydrate about 68.7 wt.%^[18].

The injection molding process utilized Polypropylene HP 550, a high fluidity homopolymer, to fabricate the workpieces. This material boasts a Shore D hardness of 71 and a density of 0.905g/cm³ at 23 °C. CAE simulations were carried out to obtain the injection molding parameters. The workpieces were characterized through microstructural analysis, tensile tests, warpage, and crystallinity degree. Thermocouples were installed inside the mold to furnish the real temperature during the injection process to add to the proposed investigation. Other peripheral analyses are also briefly discussed, which even if not deeply investigated, may contribute to future research.

2.1 Part geometry and the injection molds

The workpiece geometry consists of a disc of 140 mm in diameter, and five equidistant cavities with 28.5 mm of height, interconnected by 2 mm of thickness. A central sprue was used of 60 mm in length and 6 mm in diameter at the entrance with a draft angle of 2°. The sensor 1 was installed in the fixed cavity and the sensor 2 in the movable cavity, on the molding block, 10 mm away from plastic part

(Figure 1), in order to avoid marks on the product surface. Figure 1 shows the interchangeable inserts, the workpiece, and the entire mold. Two thermocouple type-K were installed inside the molds, as presented in Figure 1b. Both sensors were installed 10 mm away from the workpiece.

The RenShape®5166 resin is a material usually used for prototyping and other similar applications. Rapid tooling is favored for small batch injection cycles due to its advantages like reduced lead time, lower capital costs, and enhanced customization. The demand for timely delivery of low-cost products with diverse geometries is on the rise, driving its widespread adoption across industries, especially in new product development^[23]. Thus, its thermal properties are not found on its datasheet^[24]. However, to conclude the present work, the thermal properties of the RenShape had to be established. To do so, the thermal conductivity was obtained by following the ISO 8301-1991 standard, utilizing a heat flow meter apparatus with a Symmetrical Single-specimen layout. Thermal resistance was determined using Fourier's law, and the thermal conductivity was calculated by dividing the resin's thickness (50.8mm) by the thermal resistance, resulting in a value of 0.51 W/mK with an uncertainty of 4%. The resin sample was considered homogeneous.

The specific heat determination was performed using differential scanning calorimetry (DSC) equipment, specifically the TA Instruments model Q20, following the ASTM E1269 standard. At a rate of 10 °C/min, the following procedures were carried out: first with an empty crucible, the second with Sapphire as the standard, and the third with the resin of interest. The specific heat values of the empty crucible were subtracted from the reference results and the resin's specific heat values to obtain the desired outcome. The specific heat value collected at 86.85 °C, which closely represents the average surface temperature expected during the injection process, was determined to be 1648 J/kg.K.

For the AISI P20 and CuBe alloy, their thermal properties can be found on their datasheets. The density and the thermal conductivity of the three materials used to manufacture the mold's inserts are presented in Table 1.

A CNC milling machine Feller model FV-600 was utilized to machine the inserts. Figure 2 shows the final mold, the inserts, and some molded workpieces.

In a peripheral analysis, to gain a general idea about the manufacturing time considering the rapid tooling application, a simplified analysis of the manufacturing time of the inserts was conducted. The machining time was assessed and is presented in Table 2 (only the milling process). It may be considered that machining time is a very complex subject, involving cutting parameters, a CNC machine, a cutting tool, a fixture, and so on. This information is only presented to offer a first view of the machining time of these materials. It is limited to the resources used in the present work.

In the case investigated, the same cutting parameters for the P20 and CuBe were used; thus, the milling time was the same. A reduction of about 50% of the machining time was verified with the resin, because of the roughing operation. In this operation, the resin material propitiated higher cutting parameters and speeds. Figure 3 provides a view of the toolpath for roughing. Figure 3a shows the roughing for resin, a lower density of toolpaths, and Figure 3b the tool path for AISI P20, which requires a shallower cut, thus requiring more density of toolpaths, resulting in a longer machining time.

Table 1. Main properties of the tested insert materials.

Parameter	P20	CuBe alloy	Resin
Density (g/cm ³)	7.8	8.3	1.7
Thermal conductivity (W/m.K)	29	97	0.51

Table 2. Machining time of the inserts according to its material.

	Resin	AISI P20 / CuBe – same cutting parameters
Roughing	29 min	3h 40 min
Semi-finishing	46 min	46 min
Finishing	2h 12 min	2h 12 min
Total	3h 28 min	6h 38min

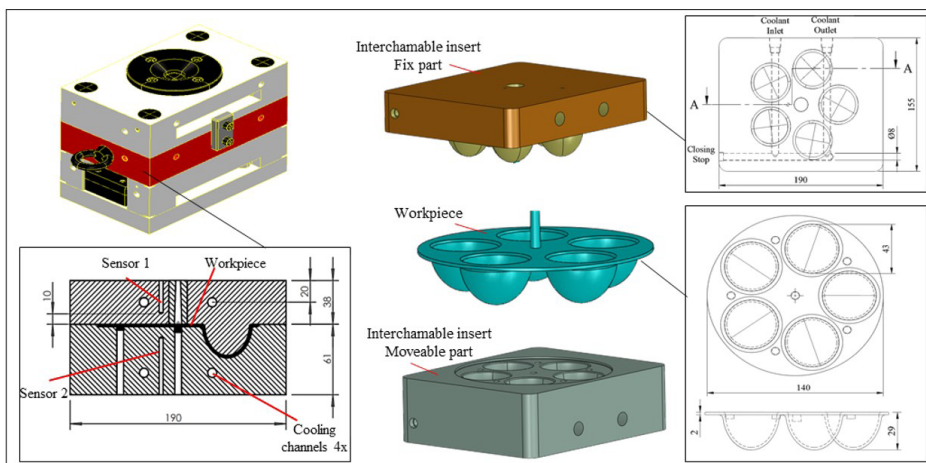


Figure 1. Workpiece geometry, inserts, entire mold, and position of the thermocouples (sensor 1 and sensor 2).

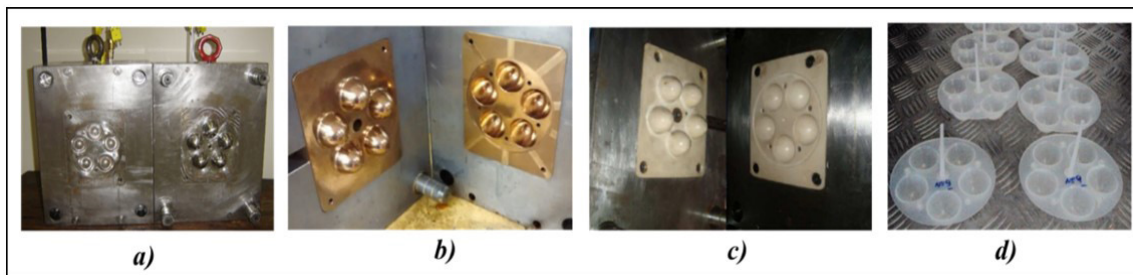
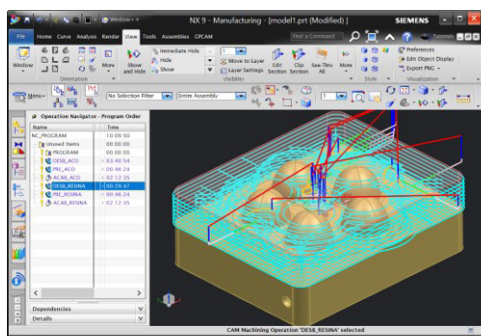
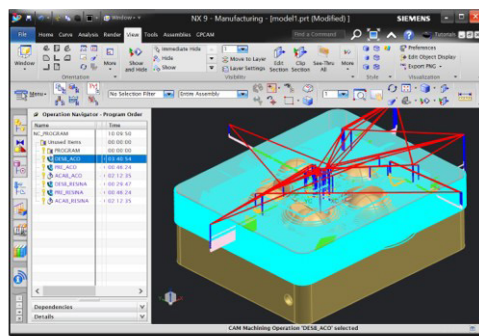


Figure 2. Mold and the different inserts. (a) P20 steel; (b) CuBe alloy; (c) resin; (d) the molded workpieces.



a) Toolpath for resin



b) Toolpaths for P20 and CuBe

Figure 3. Visualization of the toolpaths for roughing operation (NX Siemens).

2.2 Workpiece material and the injection molding process

The Braskem PP H201 polypropylene was used for the injection molding of the workpieces. The CAE software Moldflow® was used to obtain the main injection molding parameters. The simulated parameters as well as the real ones used in the experiments are presented in Table 3. A Sandretto injection molding machine model MICRO 650/247 was used for injection molding the workpieces.

Fixing the parameter of the injection molding using the AISI P20 resulted in a remarkable reduction of 46% in the cycle time using the CuBe inserts, and an increase of about 2,800% in the cycle time using the alternative resin.

2.3 Characterization of the molded workpieces

To evaluate the influences that each mold material had on the molded plastic parts, specimens were withdrawn from the injected workpieces to carry out morphology analysis and tensile test. The specimens from the workpiece were obtained from the local indicated in Figure 4.

The Olympus model BH2 microscope was utilized to observe via polarized optical images the morphology of the injected parts. A Leitz 1401 microtome was utilized to cut the samples at room temperature, with 10 μm of thickness. The formation and characteristics of the skin, the center, and the size of the spherulites were analyzed. Tensile tests were conducted according to ASTM D 638 type V (ASTM D638)^[25]. For a statistic evaluation, five specimens of ASTM D 638 type V were extracted from the workpiece, as shown in Figure 4.

Table 3. Simulated injection parameters by Moldflow® and real values used.

	Moldflow® Simulation		
	Resin	P20	CuBe
Injection Time (s)	0.7	1.06	1.06
Holding time (s)	19	4.7	4.5
Cooling time (s)	600	16.8	6.2
Cycle time (s)	619.7	22.5	11.8
Real injection parameters			
Injection Time (s)	0.7	1.7	1.1
Holding time (s)	19	4,7	4.5
Cooling time (s)	600	15	6
Cycle time (s)	622	21.4	11.6

The warpage of the injected workpiece was evaluated by measuring five points on it, which were then compared to part nominal dimension on the CAD model (28.5 mm). These points were accessed by a Mitutoyo Crista 710 coordinate measuring machine. The computer-aided inspection (CAI) system was utilized for warpage assessment. Using a coordinate measuring machine (CMM), the sample was measured at five predetermined points in a sequence (refer to Figure 4a). These values were then compared to the original ones from the 3D CAD geometry, and any differences were noted. Analysis of variance (ANOVA) was realized to evaluate the warpage among the samples.

Differential scanning calorimetry (DSC) was used to measure the degree of crystallinity of injected polypropylene.

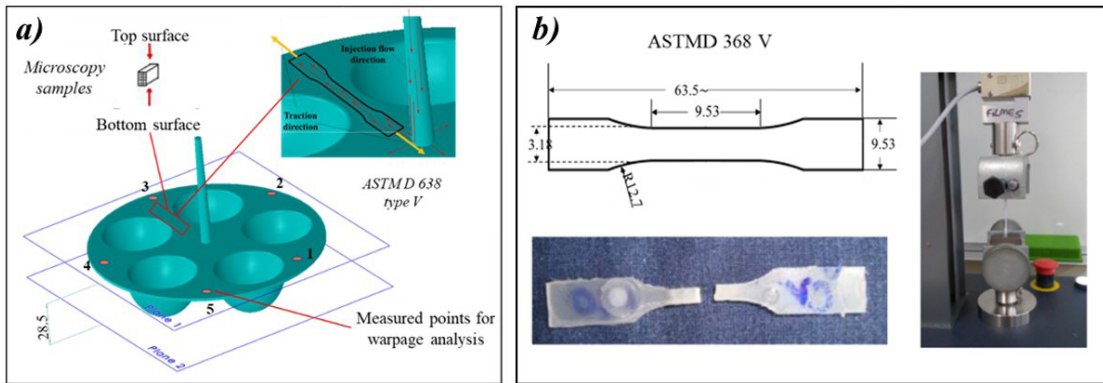


Figure 4. Workpiece and samples for analyses. (a) Schematic representation of geometry; (b) Tensile tests.

This is a satisfactory technique to assess the degree of the PP parts^[26]. TA Instruments, model Q20, was utilized, with a heating rate of 10 °C/min from 20 °C to 300 °C in an inert atmosphere of oxygen. The method consists of an energy measurement to melt the polymer crystal and compare it to the known value of 100% melt crystals using Equation 1.

$$\%C = \left(\frac{\Delta H}{\Delta H^0} \right) 100 \quad (1)$$

where (%C) is the degree of crystallinity degree of crystallinity (%), (ΔH) is the experimentally melting enthalpy for PP H201, and (ΔH^0) the theoretical enthalpy, considering (209 J·g⁻¹) as a reference value^[27]. All specimens were extracted from the same local, as shown in Figure 4.

3. Results and Discussion

Firstly, a discussion is presented about the injection molding cycle time according to the material's thermal conductivity of the inserts of the mold, to furnish a production perspective and some concerns for the following analyses. Then, the temperature behavior during the injection molding process for each pair of inserts and the analyses of microstructure, the part's warpage, crystallinity degree, and tensile tests are presented.

3.1 The cycle time according to the material's thermal conductivity

Significant differences in the injection molding cycle time were observed (Table 3), as expected, which mainly occurred during the cooling time stage as a result of the insert materials' thermal conductivity.

Aiming to reduce the injection molding cycle time, in addition to the possibility of using a material with higher thermal conductivity (CuBe for example), another alternative includes the manufacture of conformal cooling channels using metal additive manufacturing technology. Thus, a discussion emerges about which option could be more advantageous. In this scenario, Marques et al.^[22] compared CAE simulation conformal cooling channels against common linear cooling channels using a P20 steel.

Their results showed a reduction in the cycle time of about 16%. Marin et al.^[28], designed and manufactured a mold with conformal cooling using metal additive manufacturing (SLM process). Evaluating the conformal cooling mold against a conventional counterpart, the reduction of the cycle time obtained reached 36% using the mold with conformal cooling. Even considering the different conditions of these works, the present work shows that CuBe could be a strong competitor for additive manufacture for molding application when considering the cooling time.

The present work shows a reduction of 46% in the cycle time using CuBe inserts, higher than that presented by Marin et al.^[28] using additive manufacturing and conformal cooling.

3.2 Analysis of the temperature

The temperature behavior during the injection molding process using the three different pairs of inserts (AISI P20, CuBe, and resin) is presented in Figure 5. Sensor 1 was in the fixed cavities and sensor 2 in the movable cavities.

Figure 5 shows that a significant alteration of temperature cannot be observed, neither in the temperature cusps nor in the temperature gradient in each insert. Furthermore, the difference in temperatures between the inserts of the same material (sensor 1 and sensor 2) at the end of a molding cycle presented little variation (between 5 °C and 8 °C).

Instead, there is a significant difference in the time that the parts remained inside the mold before extraction. Thus, the material's thermal conductivity might influence the plastic parts and/or the molding process not by altering the process temperatures itself but due to the time that the samples remain inside the mold before extraction. The temperatures and the cycle time observed for both inserts – for the three inserts' materials evaluated – are useful for the following analyses.

3.3 Analyses of the microstructure

This section presents microstructural analysis in terms of skin thickness and the spherulite formation of H201 polypropylene specimens according to the three different inserts' materials used for the injection molding of the samples.

3.3.1 Skin thickness

Figure 6 shows the micrographs obtained by polarized light microscopy (magnification of approximately 67x) of the samples molded using the inserts of CuBe (Figure 6a), AISI P20 (Figure 6b), and resin (Figure 6c), highlighting the skin formation. Firstly, it is noticeable that the micrograph of the sample injected using the resin insert does not have well-defined layers between the skins (Figure 6c).

In general, two distinct regions can be observed on the micrograph of the injected samples, presenting morphological alterations. First, a region with a highly oriented layer in the border of the material – the skin – and a massive region in the central portion – the core. Between these regions, there is a formation of a transition zone next to the core, and a high shear zone denoted by a darkened region. However, such a transition zone cannot be observed on the samples molded by the resin inserts (Figure 6c, 40x magnified). This likely occurred because of the frozen skin together with the low thermal conductivity of the resin inserts, which resulted in a longer melt temperature in the core region propitiating more time for a molecular restructuration.

Table 4 presents the skin thickness of the molded samples. These values were obtained using the image in Figure 6 and the software ImageJ®. The materials of the inserts directly influence the total skin thickness. Higher thermal conductivity in the inserts results in a thicker skin layer. Additionally, within the same timeframe, increasing the thermal conductivity of the mold material leads to a decrease in temperature. This aligns with the established understanding that cooler molds produce thicker skins on the moldings. Conversely, higher mold temperatures allow for a longer period for the material to relax its orientation, thereby reducing the initial size of the oriented skin^[4].

A highly oriented outer layer (skin) is formed when the melted polymer contacts the cold mold, which automatically

freezes due to the high-temperature differences resulting in a solid frozen layer^[29]. However, in the present work, in the resin inserts even the real temperature was 8% colder than the CuBe ones. When the material entered the mold, the resin inserts propitiated smaller skin than the parts molded by the CuBe inserts. It is suggested that in such cases, due to the elevated total cycle time requested for the resin inserts (which took 5.261% longer), it might signify that the skin is not formed instantaneously, requiring a time interval. Given such time, if the inserts had greater thermal conductivity, it would propitiate a thicker skin. Thus, this may explain why the inserts with higher thermal conductivity and higher temperature at the beginning of the process generated parts with thicker skins.

3.3.2 The formation of the spherulites

Figure 7 shows the core formation of the spherulites. It is noticeable that the size of the spherulites increase from the CuBe compared to the resin inserts. The core of the samples is generally formed by α -type spherulitic crystallization and exhibits a Maltese cross due to the birefringent property of the material.

The size of the skin is influenced by various factors, but its final size is determined by the degree of relaxation

Table 4. Layer measurements of P20, CuBe, and resin injected samples by polarized light microscopy.

Sample layer	CuBe inserts	P20 inserts	Resin inserts
Outer layer	0.01 mm	0.02 mm	0.19 mm*
Refined layer and high shear	0.16 mm	0.08 mm	
Transition zone	0.19 mm	0.17 mm	
TOTAL	0.35 mm	0.26 mm	0.19 mm

*The micrograph analysis on the sample injected into a resin insert does not present well-defined layers.

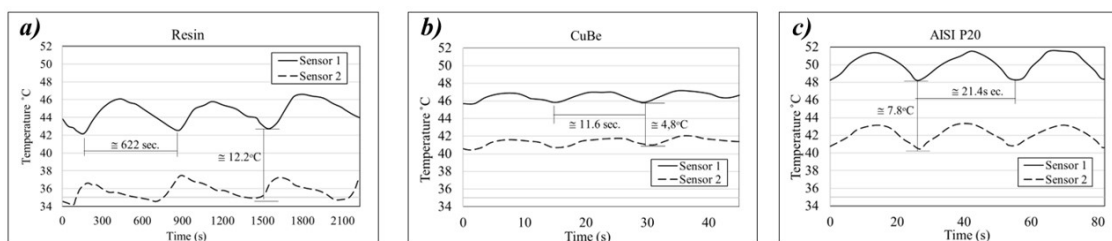


Figure 5. Temperature monitored during the injection process.

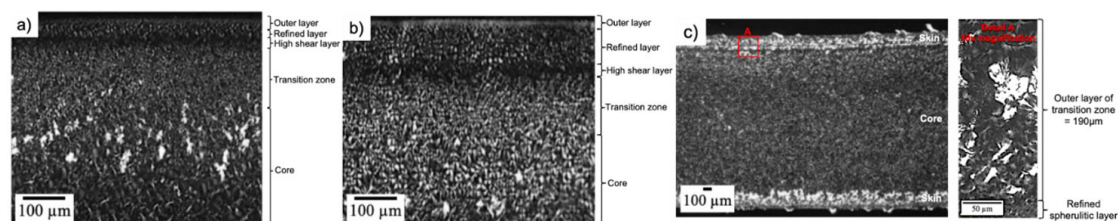


Figure 6. Micrograph of the injected samples using different insert material: (a) AISI P20; (b) CuBe; (c) Resin.

of stress-induced orientation in the material. A shorter cooling time reduces the period for the material to relax its orientation, thereby increasing the ‘original’ size of the oriented skin^[1].

According to Lee and Cha^[9], the low mold temperature of the molds’ cavities impedes the growth of the polymer cells during the melting process. A thicker skin can provide higher insulation to the core, and for that reason, the spherulites can grow in the core zone^[8].

However, by conjoining both these conclusions, the study suggests that the thermal conductivity of the mold’s inserts outweighs the importance of mold temperature and skin thickness. CuBe inserts resulted in smaller spherulites despite thicker skin (Table 4), due to rapid solidification caused by high thermal conductivity. Conversely, resin inserts with low thermal conductivity led to spherulite growth despite thinner skin and lower mold temperature. Therefore, when comparing insert materials, thermal conductivity proves more significant in determining spherulite size during formation.

3.4 Warpage analysis

The warpage was evaluated by measuring five positions on the top surface of the workpieces (Figure 8) produced by injection molding using the three inserts’ materials. Considering that the nominal value of the evaluated point is 28.50 mm (Figure 8), for a confidence interval of 95%, the samples injected in the AISI P20 insert presented an average value of 28.49 ± 0.07 mm, CuBe 28.46 ± 0.15 mm, and 28.30 ± 0.14 mm for the resin inserts, as presented in Figure 8a. The expected deformation is depicted in Figure 8b, considering the hotter and colder inserts positioned on the fixed and movable components of the injection machine, respectively.

Firstly, in a general view, the one-way analysis of variance (ANOVA) showed that there is no significant difference ($p=0.131$) in the parts’ warpage using the different inserts’ materials evaluated in the present work (AISI P20, CuBe, and resin).

Contrary to expectations, resin inserts were anticipated to reduce warpage in parts. However, despite longer cooling

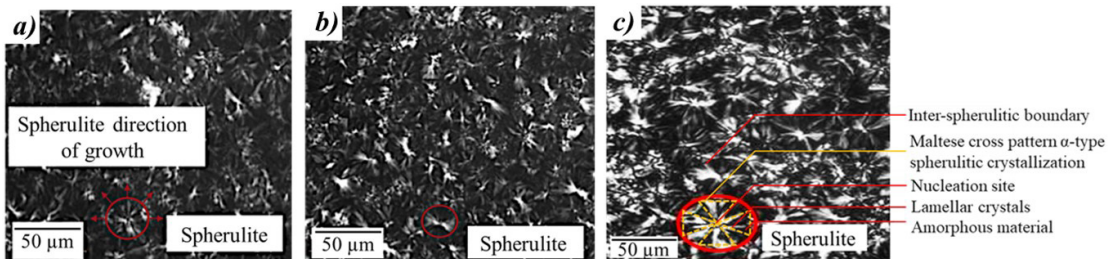


Figure 7. Micrograph of the core of the injected samples showing the spherulite and its characteristics (a) in AISI P20 steel inserts; (b) in CuBe inserts; (c) in resin.

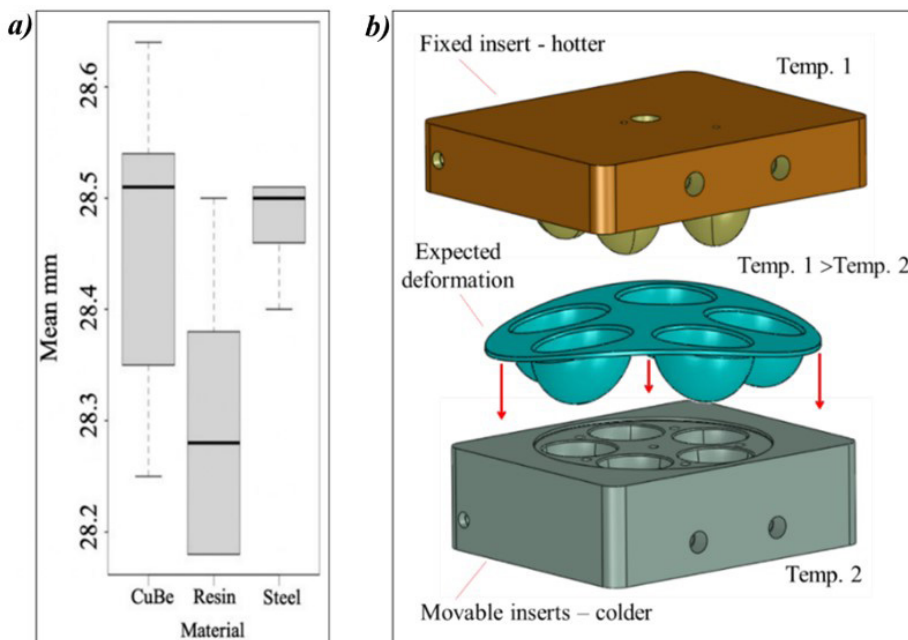


Figure 8. Warpage analysis. (a) Box plot of warpage; (b) expected deformation.

Table 5. Results of the enthalpy of fusion, degree of crystallinity, modulus of elasticity, and maximum strain of the injected samples.

Properties	Insert material		
	CuBe	AISI P20	Resin
Crystallinity	34.2%	37.8%	53.5%
Enthalpy of Fusion	71.5 J/g	79.1 J/g	111.9 J/g
Young Modulus (E) GPa	1.72 ± 0.12	1.90 ± 0.15	1.01 ± 0.22
Max Strain (MPa)	32.35 ± 0.62	35.62 ± 1.17	36.28 ± 1.35

times for samples produced using resin inserts, warpage tendencies were higher compared to counterparts. This suggests that the core portion of the sample may accumulate more residual stress, exerting a greater influence on warpage. The samples produced by the resin inserts presented smaller skin thickness (about 54% smaller than the CuBe ones), and consequently a larger volume of the core portion, which likely influenced the warpage. Therefore, the volume of the core portion may be the reason why the resin inserts, even with a longer cooling time, had the tendency to present more warpages than the others.

3.5 Degree of crystallinity and tensile test analyses

Table 5 shows the degree of crystallinity of samples injected in the present work as well as the young modulus and the maximum strain. The resin inserts produced parts with higher crystallinity and CuBe counterparts with lower crystallinity. This may occur because the resin inserts permitted a longer time of the crystalline temperature inside the mold, which occurred not because of the skin thickness (these samples had smaller skin) but due to the lower thermal conductivity of the resin inserts. The lower thermal conductivity of the inserts permits the polymer molecules to rearrange in an ordered manner within the structure, consequently increasing the degree of crystallinity, as observed in the three cases studied in the present work (the three insert materials).

For the maximum strain, the CuBe inserts presented the lowest values whereas the resin inserts resulted in the highest ones. Evaluating the properties accessed on the samples molded by resin inserts against the CuBe ones, there are: the resin inserts i) increased sizes of the spherulites, ii) a 56% increase in the crystallinity degree, and iii) a 45% reduction in the skin thickness. All these properties increased the maximum strain of the parts manufactured by resin inserts by 12%. From perspective of the skin thickness, a reduction of skin thickness increased the maximum strain. Thus, this may mean that skin thickness can represent a weak structure, based on the maximum strain evaluation. The thinner the skin, the more material is required in the core portion of the part.

Considering the young modulus, firstly, the larger spherulite structure found in the core of the molded parts using the resin inserts (Figure 7c) may contribute to reducing the young modulus due to the lower number of secondary bounds among the spherulites, in comparison with the structure observed on the samples produced by the others inserts. Secondly, all the refined skin layers were formed, in this work, on the polymer flow direction during the filling stage and is coincident with the direction

of the traction for the tensile tests (Figure 4). This is likely in relation to the young modulus. The thinner the skin, the lesser young modulus are present. This fact can be verified by the samples molded by the resin inserts.

4. Conclusions

This study explores the influences of the materials used to manufacture injection molding inserts, focusing on either reducing the molding cycle time or the time and costs to manufacture the inserts (rapid tooling). To do so, three pairs of inserts were manufactured: i) the ordinary AISI P20 (as a reference), ii) CuBe alloy (due to reduce molding time by its high thermal conductivity), and iii) ReniShape resin (savings on the manufacture of the mold for small batch production of plastic parts, rapid tooling). These three pairs of inserts were used for injection molding in the PP parts. The mold manufacturing and the injection molding process were assessed, and the properties of the molded parts were examined using these different mold materials.

Key findings include a 46% reduction in injection molding cycle time with CuBe inserts compared to AISI P20. In contrast, Marin et al.^[28] found a reduction of about 36% in cycle time using injection molds with conformal cooling channels manufactured by additive manufacturing technology (high cost/time). Thus, the results observed in the current study hold significant potential for using CuBe inserts to reduce the costs and requirements associated with additive manufacturing process. Despite minimal temperature variations (5-8 °C), skin thickness dynamics, spherulite formation, and unexpected warpage tendencies were observed. The study suggests using CuBe inserts and outlines future research directions. CuBe inserts yield smaller spherulites due to rapid solidification and high conductivity.

The use of alternative resin Renishape reduced more than 50% the machining time of the mold's inserts, on the other hand, it increased 2,800% in molding cycle time. In the plastic parts, the resin inserts promoted spherulite growth due to lower conductivity and gradual cooling of the melt.

Regarding the skin thickness, the resin inserts yield thinner skins. The longer cycle time required by the resin inserts suggests that the skin formation may not occur instantaneously, requiring a time interval. If the inserts had higher thermal conductivity, it could lead to thicker skin formation. This explains why inserts with higher thermal conductivity and temperature at the beginning of the process produced parts with thicker skins.

The ANOVA analysis showed no significant warpage difference among AISI P20, CuBe, and resin-insert parts. Contrary to the literature, longer cooling times in resin-insert samples led to a higher warpage tendency, possibly due to thinner skins causing a larger core volume and concentrated residual stress.

Suggested future work: (1) Use computational simulation to analyze the impact of mold inserts on part properties; (2) Evaluate wear resistance in different insert materials; (3) Conduct a comprehensive cost-benefit analysis of CuBe inserts versus molds with additive manufacturing (SLM) conformal cooling.

5. Author's Contribution

- **Conceptualization** – Adriano Fagali de Souza; Janaina Lisi Leite Howarth.
- **Data curation** – Bruno Edu Arendarchuck; Alexandre Mateus Popiolek; Claudio Antonio Treml Junior; Crislaine Kavilha.
- **Formal analysis** – Bruno Edu Arendarchuck; Alexandre Mateus Popiolek; Claudio Antonio Treml Junior; Crislaine Kavilha.
- **Funding acquisition** – Adriano Fagali de Souza; Janaina Lisi Leite Howarth.
- **Investigation** – Bruno Edu Arendarchuck; Alexandre Mateus Popiolek; Claudio Antonio Treml Junior; Crislaine Kavilha.
- **Methodology** – Adriano Fagali de Souza; Janaina Lisi Leite Howarth.
- **Project administration** – Adriano Fagali de Souza; Janaina Lisi Leite Howarth.
- **Resources** – NA.
- **Software** – Bruno Edu Arendarchuck; Alexandre Mateus Popiolek; Claudio Antonio Treml Junior; Crislaine Kavilha.
- **Supervision** – Adriano Fagali de Souza; Janaina Lisi Leite Howarth.
- **Validation** – Bruno Edu Arendarchuck; Alexandre Mateus Popiolek; Claudio Antonio Treml Junior; Crislaine Kavilha.
- **Visualization** – Bruno Edu Arendarchuck; Alexandre Mateus Popiolek; Claudio Antonio Treml Junior; Crislaine Kavilha.
- **Writing – original draft** – Adriano Fagali de Souza; Bruno Edu Arendarchuck; Alexandre Mateus Popiolek.
- **Writing – review & editing** – Adriano Fagali de Souza; Bruno Edu Arendarchuck; Alexandre Mateus Popiolek.

6. Acknowledgements

The authors would like to thank The National Council for Scientific and Technological Development (CNPq) for the doctorate scholarship and the Fellow Researcher Funding (306438/2021-6), and the Fundação de Amparo a Pesquisa e Inovação de Santa Catarina (FAPESC) for the financial support of this research.

7. References

1. Chen, J.-Y., Tseng, C.-C., & Huang, M.-S. (2019). Quality indexes design for online monitoring polymer injection molding. *Advances in Polymer Technology*, 2019, 3720127. <http://doi.org/10.1155/2019/3720127>.
2. Marin, F., Souza, A. F., Ahrens, C. H., & de Lacalle, L. N. L. (2021). A new hybrid process combining machining and selective laser melting to manufacture an advanced concept of conformal cooling channels for plastic injection molds. *International Journal of Advanced Manufacturing Technology*, 113(5-6), 1561-1576. <http://doi.org/10.1007/s00170-021-06720-4>.
3. Bozdana, A. T., & Eyercioğlu, Ö. (2002). Development of an expert system for the determination of injection moulding parameters of thermoplastic materials: EX-PIMM. *Journal of Materials Processing Technology*, 128(1-3), 113-122. [http://doi.org/10.1016/S0924-0136\(02\)00436-3](http://doi.org/10.1016/S0924-0136(02)00436-3).
4. Brito, A. M., Cunha, A. M., Pouzada, A. S., & Crawford, R. J. (1991). Predicting the skin-core boundary location in injection moldings. *International Polymer Processing*, 6(4), 370-377. <http://doi.org/10.3139/217.910370>.
5. Farotti, E., & Natalini, M. (2018). Injection molding: influence of process parameters on mechanical properties of polypropylene polymer: a first stud. *Procedia Structural Integrity*, 8, 256-264. <http://doi.org/10.1016/j.prostr.2017.12.027>.
6. Altaf, K., Rani, A. M. A., Ahmad, F., Baharom, M., & Raghavan, V. R. (2016). Determining the effects of thermal conductivity on epoxy molds using profiled cooling channels with metal inserts. *Journal of Mechanical Science and Technology*, 30(11), 4901-4907. <http://doi.org/10.1007/s12206-016-1055-z>.
7. Viana, J. C. (2004). Development of the skin layer in injection moulding: phenomenological model. *Polymer*, 45(3), 993-1005. <http://doi.org/10.1016/j.polymer.2003.12.001>.
8. Karger-Kocsis, J., & Bárányi, T. (Eds.). (2019). *Polypropylene handbook: morphology, blends and composites*. Switzerland: Springer. <http://doi.org/10.1007/978-3-030-12903-3>.
9. Lee, J. J., & Cha, S. W. (2006). Characteristics of the skin layers of microcellular injection molded parts. *Polymer-Plastics Technology and Engineering*, 45(7), 871-877. <http://doi.org/10.1080/03602550600611768>.
10. Baltés, L., Costiuc, L., Patachia, S., & Tiorean, M. (2019). Differential scanning calorimetry: a powerful tool for the determination of morphological features of recycled polypropylene. *Journal of Thermal Analysis and Calorimetry*, 138(4), 2399-2408. <http://doi.org/10.1007/s10973-019-08679-7>.
11. Strömberg, E., & Karlsson, S. (2009). The design of a test protocol to model the degradation of polyolefins during recycling and service life. *Journal of Applied Polymer Science*, 112(3), 1835-1844. <http://doi.org/10.1002/app.29724>.
12. Rizvi, S. J. A. (2017). Effect of injection molding parameters on crystallinity and mechanical properties of isotactic polypropylene. *International Journal of Plastics Technology*, 21(2), 404-426. <http://doi.org/10.1007/s12588-017-9194-3>.
13. van Renterghem, J., Dhondt, H., Verstraete, G., De Bruyne, M., Vervae, C., & De Beer, T. (2018). The impact of the injection mold temperature upon polymer crystallization and resulting drug release from immediate and sustained release tablets. *International Journal of Pharmaceutics*, 541(1-2), 108-116. <http://doi.org/10.1016/j.ijpharm.2018.01.053>. PMID:29409747.
14. Suplicz, A., Szabo, F., & Kovacs, J. G. (2013). Injection molding of ceramic filled polypropylene: the effect of thermal conductivity and cooling rate on crystallinity. *Thermochimica Acta*, 574, 145-150. <http://doi.org/10.1016/j.tca.2013.10.005>.
15. Sperling, L. H. (2005). *Introduction to physical polymer science*. Hoboken: John Wiley & Sons. <http://doi.org/10.1002/0471757128>.
16. Cowie, J. M. G., & Arrighi, V. (2007). *Polymers: chemistry and physics of modern materials*. Boca Raton: CRC Press. <http://doi.org/10.1201/9781420009873>.
17. Menges, G., Michaeli, W., & Mohren, P. (2001). *How to make injection molds*. Munich: Hanser.
18. Fernandes, A. C., Souza, A. F., & Howarth, J. L. L. (2016). Mechanical and dimensional characterization of polypropylene injection moulded parts in epoxy resin/aluminium inserts for rapid tooling. *International Journal of Materials & Product Technology*, 52(1-2), 37-52. <http://doi.org/10.1504/IJMPT.2016.073618>.
19. Beal, V. E., Erasenthiran, P., Ahrens, C. H., & Dickens, P. (2007). Evaluating the use of functionally graded materials inserts produced by selective laser melting on the injection moulding of plastics parts. *Proceedings of the Institution of Mechanical*

- Engineers. Part B, Journal of Engineering Manufacture*, 221(6), 945-954. <http://doi.org/10.1243/09544054JEM764>.
20. Apacki, K. C. (1995). *Copper-alloy molds provide cycle time and quality advantages for injection molding and resin transfer molding* (SAE Technical Paper, No. 950566). Warrendale: SAE International. doi:<http://doi.org/10.4271/950566>.
 21. Kelly, A. L., Mulvaney-Johnson, L., Beechey, R., & Coates, P. D. (2011). The effect of copper alloy mold tooling on the performance of the injection molding process. *Polymer Engineering and Science*, 51(9), 1837-1847. <http://doi.org/10.1002/pen.21975>.
 22. Marques, S., Souza, A. F., Miranda, J., & Yadroitsau, I. (2015). Design of conformal cooling for plastic injection moulding by heat transfer simulation. *Polimeros*, 25(6), 564-574. <http://doi.org/10.1590/0104-1428.2047>.
 23. Huzaim, N. H. M., Rahim, S. Z. A., Musa, L., Abdellah, A. E., Abdullah, M. M. A. B., Rennie, A., Rahman, R., Garus, S., Błoch, K., Sandu, A. V., Vizureanu, P., & Nabialek, M. (2022). Potential of rapid tooling in rapid heat cycle molding: a review. *Materials (Basel)*, 15(10), 3725. <http://doi.org/10.3390/ma15103725>. PMID:35629751.
 24. Huntsman Advanced Materials. (2007, June 3). RenShape® 5166: datasheet. Switzerland: Huntsman Advanced Materials Americas Inc.
 25. American Society for Testing and Materials – ASTM. (2022). *ASTM D638-22: standard test method for tensile properties of plastics*. West Conshohocken: ASTM International.
 26. Kong, Y., & Hay, J. N. (2003). The enthalpy of fusion and degree of crystallinity of polymers as measured by DSC. *European Polymer Journal*, 39(8), 1721-1727. [http://doi.org/10.1016/S0014-3057\(03\)00054-5](http://doi.org/10.1016/S0014-3057(03)00054-5).
 27. Ujhelyiová, A., Horbanová, L., Petková, M., Ryba, J., & Annus, J. (2019). Polypropylene crystallisation in the presence of inorganic additives. *Fibres & Textiles in Eastern Europe*, 27(2), 30-38. <http://doi.org/10.5604/01.3001.0012.9984>.
 28. Marin, F., Miranda, J. R., & Souza, A. F. (2018). Study of the design of cooling channels for polymers injection molds. *Polymer Engineering and Science*, 58(4), 552-559. <http://doi.org/10.1002/pen.24769>.
 29. Callister, W. D., Jr., & Rethwisch, D. G. (2018). *Materials science and engineering: an introduction*. Brisbane: John Wiley & Sons.

Received: Jan. 02, 2024

Revised: Mar. 28, 2024

Accepted: May 08, 2024